SUPPLEMENTAL MATERIAL

Supplemental Materials and Methods

Mouse generation and breeding

All mouse experiments were approved by the HMRI Institutional Animal Care and Use Committee (IACUC).

To generate *LoxP-Apoa1bp* mice, a vector including 4 Kb 5' upstream, the whole 6 exons and 2 Kb 3' downstream of *Apoa1bp* gene was constructed and used for targeting B6 ES cells. The ES cell clones that had legitimate LoxP-Apoa1bp homologous recombination were further verified with chromosome counting, and two were selected and transplanted into the blastocyst to generate floxed *Apoa1bp* chimeras, which were crossed with B6 Albino to obtain germline-transmitted *Loxp-Apoa1bp* mice. The floxed *Apoa1bp* mice were crossbred with CMV-Cre mice to produce global AIBP knockout mice, which were backcrossed with B6 mice to remove Cre. *Apoa1bp*$^{-/-}$*ApoA1*^{Tg} mice were generated by crossing the *Apoa1bp*$^{-/-}$ mice with *ApoA1*^{Tg} mice (JAX).

Quantitative RT-PCR

Total RNA from the retina was extracted using a MiniPrep kit (Zymo Research) and reversely transcribed to cDNA (qScript; Quanta Biosciences) in a Miniopticon thermal cycler (Bio-Rad, C1000 Touch) following the manufacturer's instructions. The qRT-PCR products were measured using SYBR green-based detection (Applied Biosystems). The relative expression levels of the different genes were calculated based on the Ct values obtained for the gene of interest and 18S rRNA (the internal control).

The primers were designed using Primer3 software (http://frodo.wi.mit.edu/) as following: mouse Hes1, sense: 5'-CCAGCCAGTGTCAACACGA-3', anti-sense: 5'-AATGCCGGGAGCTATCTTTCT-3'; mouse Hey1, sense: 5'-GCGCGGACGAGAATGGAAA-3', anti-sense: 5'-TCAGGTGATCCACAGTCATCTG-3'; mouse Hey2, sense: 5'-AAGCGCCCTTGTGAGGAAAC-3', anti-sense: 5'-GGTAGTTGTCGGTGAATTGGAC-3'; mouse Nrarp, sense: 5'-TTCAACGTGAACTCGTTCGGG-3', anti-sense: 5'-TTGCCGTCGATGACTGACTG-3'; mouse Dll1, sense: 5'-CAGGACCTTCTTTCGCGTATG-3', anti-sense: 5'-AAGGGGAATCGGATGGGGTT-3', mouse Dll4, sense: 5'-TTCCAGGCAACCTTCTCCGA-3', anti-sense: 5'-ACTGCCGCTATTCTTGTCCC-3'; mouse Notch1, sense: 5'-GATGGCCTCAATGGGTACAAG-3', anti-sense: 5'-TCGTTGTTGTTGATGTCACAGT-3'; mouse Notch4, sense: 5'-CTCTTGCCACTCAATTTCCCT-3', anti-sense: 5'-TTGCAGAGTTGGGTATCCCTG-3'; mouse CD31, sense: 5'-ACGCTGGTGCTCTATGCAAG-3', anti-sense: 5'-TCAGTTGCTGCCCATTCATCA-3'; mouse VE-Cadherin, sense: 5'-CACTGCTTTGGGAGCCTTC-3', anti-sense: 5'-GGGGCAGCGATTCATTTTTCT-3'; mouse RPS18, sense: 5'-AGTTCCAGCACATTTTGCGAG-3', anti-sense: 5'-TCATCCTCCGTGAGTTCTCCA-3'

ISH riboprobe Synthesis

Digoxigenin-labeled and fluorescein-incorporated riboprobes were generated as described [1, 2]. Briefly, a RNA synthesis system containing 1 µg of linearized template DNA, 2 µl 10× concentrated DIG-NTP or Fluorescein-NTP labeling mixture (Sigma Aldrich), 2 µl 10× concentrated transcription buffer, and 2 µl (40 U) T7 RNA polymerase (NEB) were prepared and incubated was at 37°C for 2 hours. The DNA template was digested by addition of 2 µl (20 U) DNase, RNase-free (NEB) and incubation for a further 15 min at 37°C. The synthesized RNA was precipitated with 2.4 µl LiCl (4 M) in the presence of 75 µl prechilled ethanol. The precipitates were left for at least 30 min at -70°C or 2 hours at -20°C. The precipitates were spun down, washed with cold ethanol (70% [v/v]), air-dried and dissolved in RNase-free water.

Western blot

Immunoblot was done as previously described [3]. In brief, the murine retinal tissues were homogenized on ice using a Manual Disperser (PT 1200E) in the lysis buffer containing 25 mM Tris-HCl (pH 7.4), 150 mM NaCl, 1 mM EDTA, 1% NP-40, 10% glycerol supplemented with complete protease inhibitor cocktail (Thermo Scientific). Cells were washed with ice-cold PBS (pH 7.4) and then lysed. The lysates were centrifuged at maximum speed for 15 min at 4 °C. Fifty μg cell lysates were prepared for SDS-PAGE analysis (Bio-Rad). The proteins were subsequently transferred to PVDF membrane, which was blocked with 5% non-fat milk, and then incubated with primary antibodies overnight at 4°C, and further incubated with corresponding secondary antibodies, with 3 times of TBST wash after each antibody incubation. Blots were captured with a chemiluminescence detection system (ECL prime, GE Healthcare) in FluorChem M system (FM 0510, ProteinSimple).

HDL_3 isolation

HDL_3 isolation was carried out as described [4]. Fresh plasma from healthy donors was obtained from the blood bank of HMRI. A plasma density of 1.12 g/mL was prepared with KBr and used for ultracentrifugation at 35,000 rpm for 2 days at 4°C (ThermoFisher Sorvall WX 80). The lower portion of the first spin containing HDL was used to prepare a KBr density of 1.21 g/mL and centrifuged at 40, 000 rpm for 3 days at 4°C. The HDL_3 fraction was collected and dialyzed against PBS and 2 mmol/L EDTA. The purity of HDL_3 was verified with SDS-PAGE gel separation followed by Coomassie Blue staining. HDL_3 preparations were tested for possible endotoxin contamination using a LAL kit (ThermoFisher). The HDL_3 used for cell culture experiments contained endotoxin levels lower than 50 pg/mg proteins, corresponding to 2.5 pg/ml.

Cell culture

HEK-293 cells were obtained from ATCC and cultured in Dulbecco's Modified Eagle's medium (DMEM, Life Technology) containing 10% fetal bovine serum (FBS, Thermo Scientific), 100 units/ml penicillin and 100 μg/ml streptomycin (Lonza) in humidified incubator at 37 °C with 5% CO_2. HUVECs and HRMECs were purchased from Lonza and cultured in Endothelial Basal Medium (EBM_2) with 2% FBS and all supplements as well as growth factors that contained in the Bulletkit at 37 °C with 5% CO_2.

AIBP binding to HRMECs

AIBP was biotinylated as previously described [5]. Approximately 2×10^4 cells HRMECs were plated in a ZellkulTuR microplate 96-well plate (Greiner) and cultured for 2 days at 37°C humidified incubator, and the same amount of cells were plated in a transplant 96-well plate to ensure cell confluence when carrying out the assay. The biotinylated AIBP, starting from 100 μg/ml and serially diluted in EBM2-1%BSA, were incubated with HRMECs for 2 hours on ice. The cells were then washed 3 times with PBS, fixed with 4% PFA for 15 min at room temperature, and were further incubated with neutrAvidin-alkaline phosphatase (Jackson ImmunoResearch) for 30 min. After 3 washes with PBS and 3 washes with deionized water, a lumiphos 530 (Lumigen, Southfield, MI) substrate were added and the results were measured using a Tecan Infinite M1000 pro. Data were expressed as relative light units counted per 100 ms, with triplicates for each concentration. The Kd of AIBP binding to HRMECs were calculated using a total and non-specific binding algorithm of the GraphPad Prism 5.0 software.

Detergent-free isolation of lipid rafts

Lipid rafts were isolated using a detergent-free, discontinuous gradient ultracentrifugation method as previously described [6]**.** Briefly, human ECs were washed twice with ice-cold PBS and cells were scraped from the plate in 0.5 M sodium carbonate buffer (pH 11.0) containing protease inhibitor cocktail (Sigma), homogenized and sonicated for 3 × 10 sec. A 90% sucrose (w/v) solution in MBS (25 mM Mes, 0.15 M NaCl, pH 6.5) was used to adjust samples to 45% sucrose (w/v) in ultracentrifugation tubes. The 35% and 5% sucrose solutions were added consecutively to the mixture. After ultracentrifugation at 35×10^3 rpm for

20 hours at 4°C in a SW-41 rotor (Beckman), a discontinuous sucrose density gradient of 5-35% was generated. Eleven 1 ml fractions were collected from the top to the bottom of each gradient. Equal volumes of each faction (adjust to the same protein concentration) were analyzed by SDS-PAGE with presenilin1 (Cell Signaling Technology) and Notch1 (BD Biosciences) Abs.

Free cholesterol measurement
Total lipids were extracted from the cells and free cholesterol levels were measured according to the manufacture's protocol (BioVision).

γ-secretase-mediated Notch cleavage in HEK293 cells
We followed an established protocol for DLL4 treatment [7, 8]. HEK-293 cells seeded in 6-cm dishes were transiently transfected with NotchΔE construct which lacks extracellular domain of the protein and possesses only the γ-secretase cleavage site (Addgene). Experiments were performed in the presence of AIBP, HDL_3, or other chemicals as above mentioned. Western blot was used to detect γ-secretase-dependent generation of NICD.

DAPT administration
DAPT, an γ-Secretase inhibitor, was purchased from Cayman Chemicals and were dissolved in DMSO. At P4, DAPT or DMSO was injected s.c, above the eyes, with a dose of 50 mg/kg per mouse as described[9]. Twenty-four hours later (P5), retinas were analyzed using CD31 or Isolectin B4 staining.

Fluorescein angiograph

Mice were anesthetized by intraperitoneal (IP) injection of a combination of ketamine (65–100 mg/kg), xylazine (10–20 mg/kg), and acepromazine (1–3 mg/kg). Pupils were dilated with 1% tropicamide (Bausch & Lomb, Incorporated, Rochester, NY, USA). Fluorescein sodium (AK-FLUOR, 10 mg/kg, Akorn, Inc.) was delivered into mice by tail vein injection. Immediately after injection, FA was recorded using Heidelberg Retina Angiograph (HRA)-OCT device (Spectralis) from Heidelberg Engineering (Heidelberg, Germany) as described previously [10, 11].

***In vivo* Matrigel angiogenesis assay**
A mixture containing 500μl of Matrigel (BD Biosciences), 50 ng/ml VEGF (R&D) and 30 U/ml heparin (Sigma) was subcutaneously injected into the dorsal surface of *Apoa1bp*$^{-/-}$ and control mice. Two Matrigel plugs were implanted per mouse. Five days later, the mice were sacrificed and the Matrigel plugs were retrieved, processed where appropriate, and analyzed accordingly.

Murine hindlimb ischemia model
The hindlimb ischemia was performed in 9-month old male control or AIBP KO mice as previously reported with slight modification [12, 13]. Briefly, unilateral hindlimb ischemia was induced by ligating the femoral artery and its major branches. Afterwards, the mice were housed individually and blood flow in the affected and control limbs was imaged every 3 days. Total capillary density of the ischemic hindlimb cross sections was determined by staining the slides with rabbit anti-mouse CD31 (BD Biosciences), followed by horseradish peroxidase–conjugated secondary antibody.

Laser Doppler measurement of vascular perfusion
Blood flow to the ischemic or normal (nonischemic) hindlimb was examined with the use of a PeriScan PIM3 laser Doppler system (Perimed AB, Sweden), as described previously [12, 13]. Animals were prewarmed to a core temperature of 37.5°C, and heart rate was closely monitored for signs of stress from overheat. Hindlimb blood flow was measured preoperatively and postoperatively on the selected days (0, 3, 7, 10 and 14). The level of perfusion in the ischemic and normal hindlimbs was quantified with the use of the mean pixel value within the region of interest, and the relative changes in hindlimb blood flow

were expressed as the ratio of the left (ischemic) over right (normal) Laser Doppler-detected blood perfusion.

Human heart tissue collection

Fresh cardiac tissues were obtained from the surgeon under a Houston Methodist IRB-approved study during Left Ventricular Assist Device insertion for patients. A small piece of scar-free left ventricle apex samples were obtained and PFA-fixed immediately, dissected and paraffin-embedded for histological analysis. Normal hearts were from donors that were not optimal for transplantation. The 3 patients were 36 years old female, 52 years old female and 43 years old male.

Statistical analysis

Statistical analysis was carried out using Prism or Microsoft Excel. Statistical significance, otherwise specified, was determined by unpaired two-sided *t* tests. In all figures: #, not significant; *$p < 0.05$; **$p < 0.01$; ***$p < 0.001$.

Online Figures

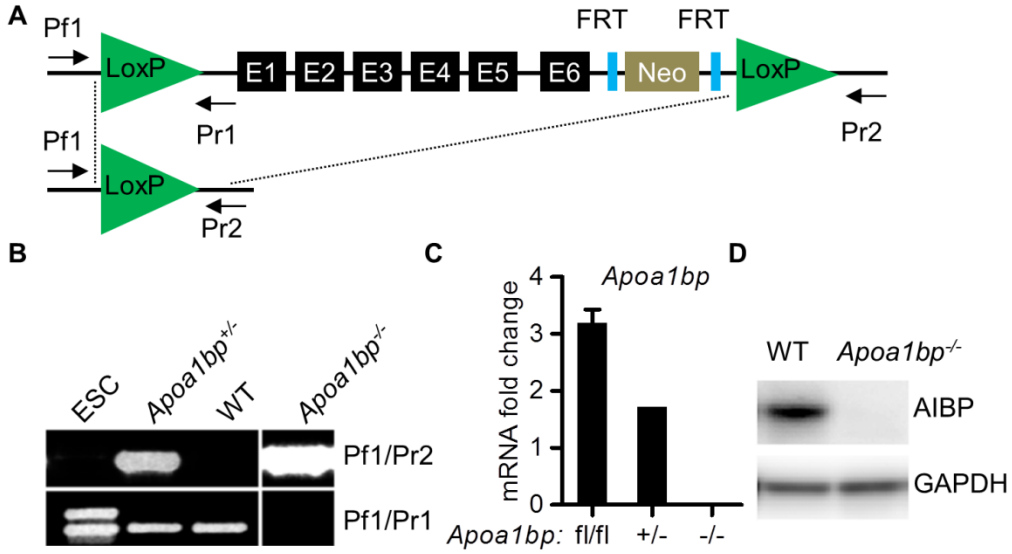

Online Figure I. Generation of *Apoa1bp* knockout mice. (A) The construct used to make an *Apoa1bp*$^{fl/fl}$ mouse. E: exon. (B) PCR genotyping of genomic DNA from positive embryonic stem cells (ESC), *Apoa1bp*$^{+/-}$ mice and *Apoa1bp*$^{-/-}$ mice. (C) Total RNA was extracted from white blood cells of *Apoa1bp*$^{fl/fl}$, *Apoa1bp*$^{+/-}$ and *Apoa1bp*$^{-/-}$ mice, and mRNA level of *Apoa1bp* was examined by qRT-PCR. (D) Western blot analysis of white blood cell lysates from *Apoa1bp*$^{-/-}$ mice and control animals.

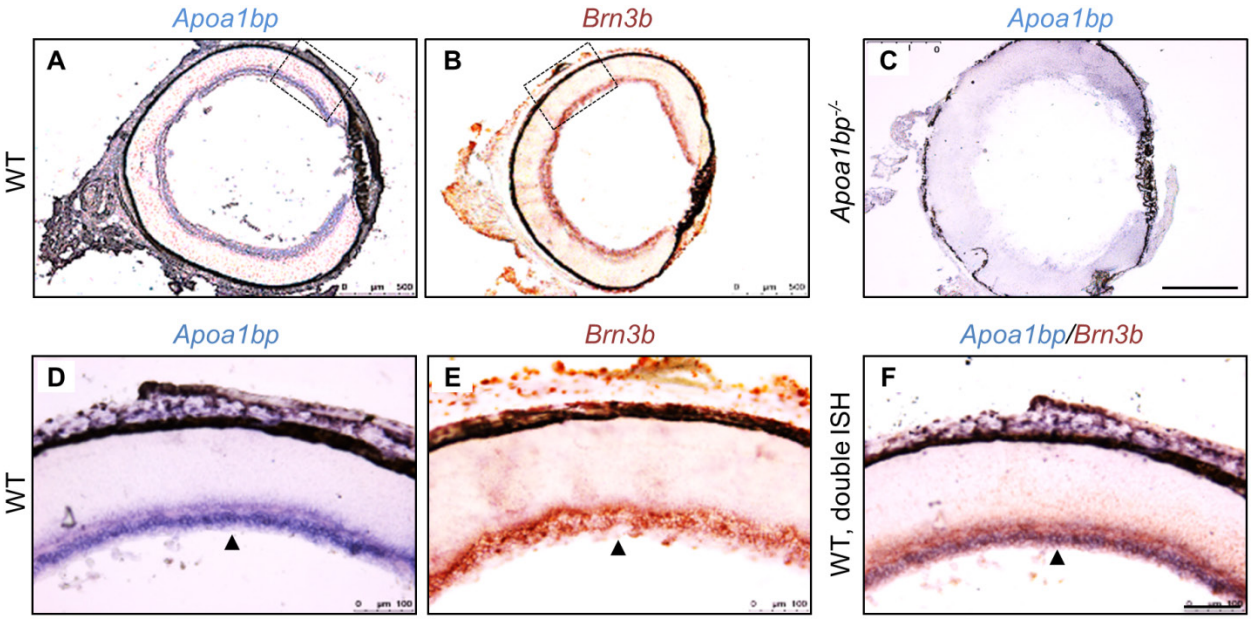

Online Figure II. AIBP localization in the murine retinas.

ISH on frozen sections of P5 retinas. Representative ISH images of two adjacent sections for *Apoa1bp* (A) and *Brn3* (B). (C) ISH of *Apoa1bp* in an AIBP knockout retina. (D and E) Enlarged images of the dash line rectangles marked in A and B. (F) ISH for both *Apoa1bp* (blue) and *Brn3* (red) on the same section. In all the panels, arrow heads depict positive ISH signal in the RGC layer. Scale bar: A–C: 500 μm; D–F: 100 μm.

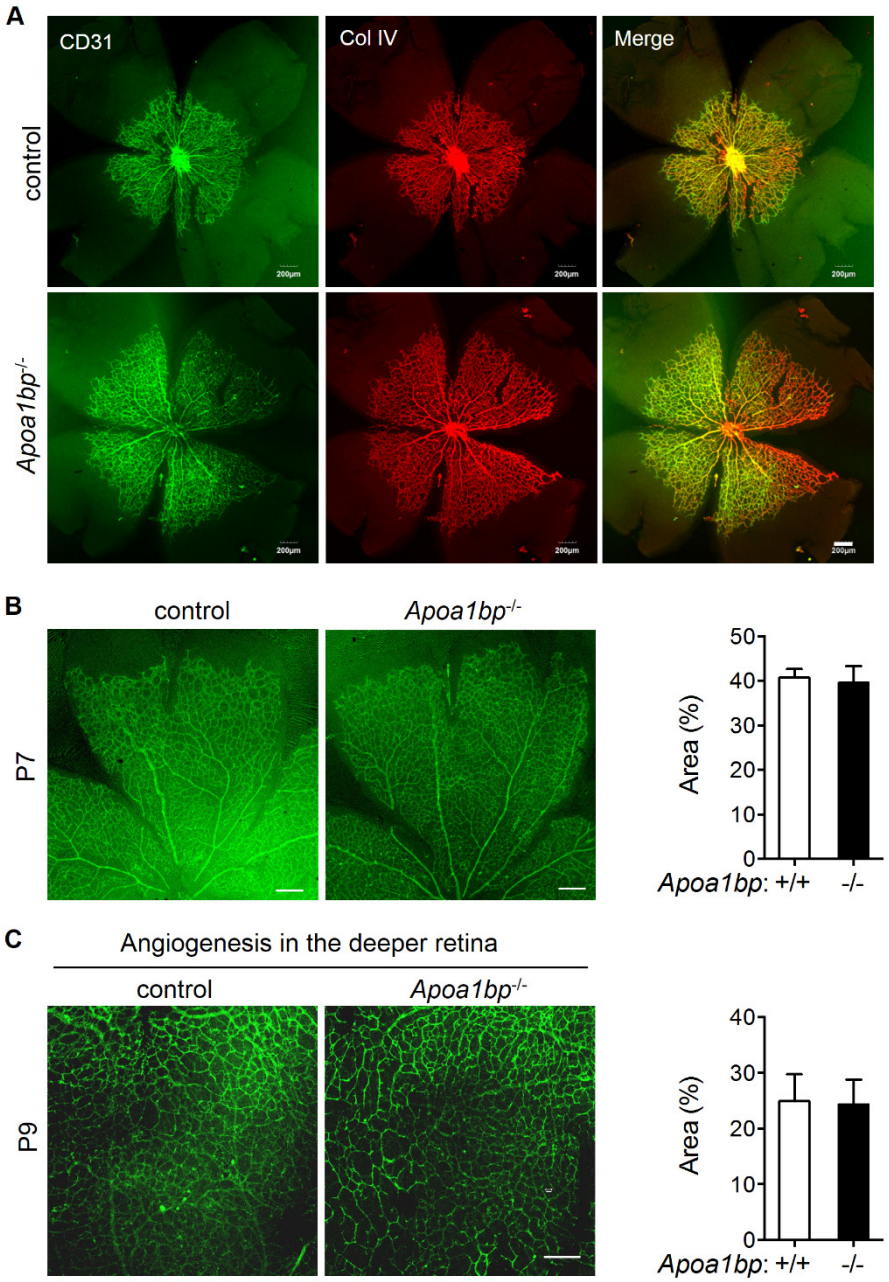

Online Figure III. Analysis of retinal angiogenesis.

Images of whole mount immunostaining of P3 retinas (A), P7 retinas (B) and P9 reitnas (C) from *Apoa1bp*$^{-/-}$ and control littermates using CD31 (green) with or without Col IV (red) antibodies. Scale bar: 200 μm; Mean ± SD; n=3.

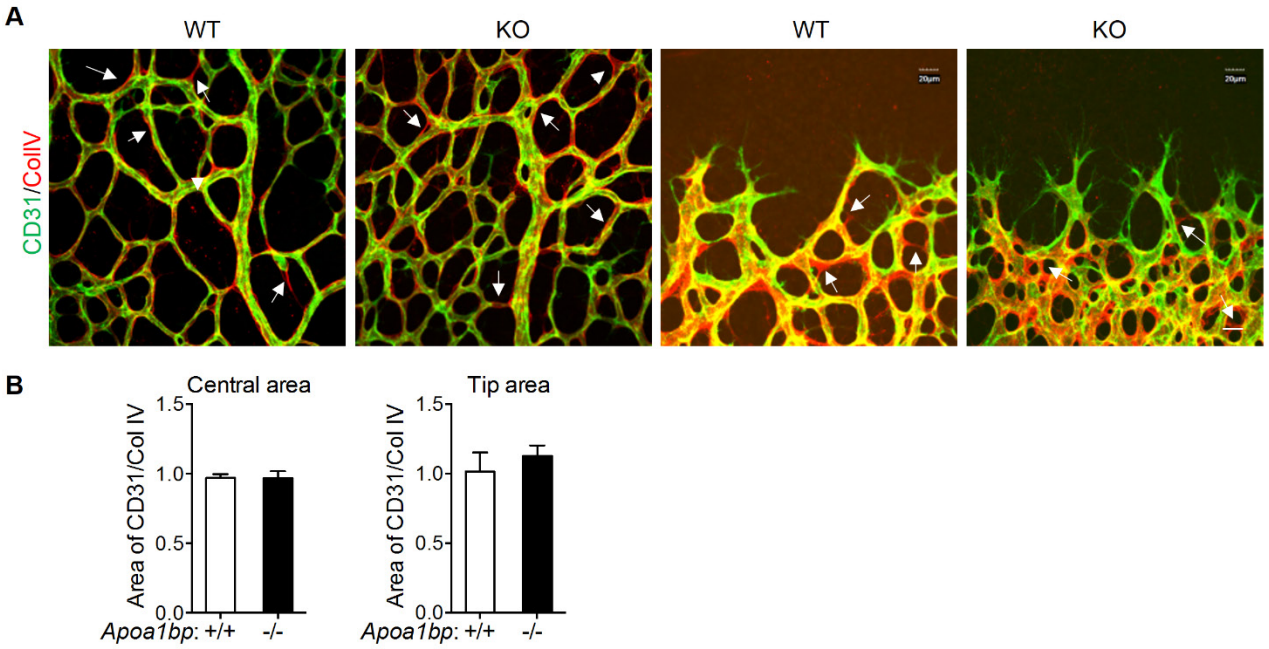

Online Figure IV. Normal vascular remodeling in AIBP KO mice. (A) Images of whole mount immunostaining of P5 retinas from *Apoa1bp*$^{-/-}$ and control littermates using CD31 (green) and Col IV (red) antibodies. (B) CD31^{+} vs. Col IV^{+} area were compared. No significant difference of vascular remodleing between control and AIBP KO retinas were found. Scale bar, 20 μm. Mean ± SD; n=3.

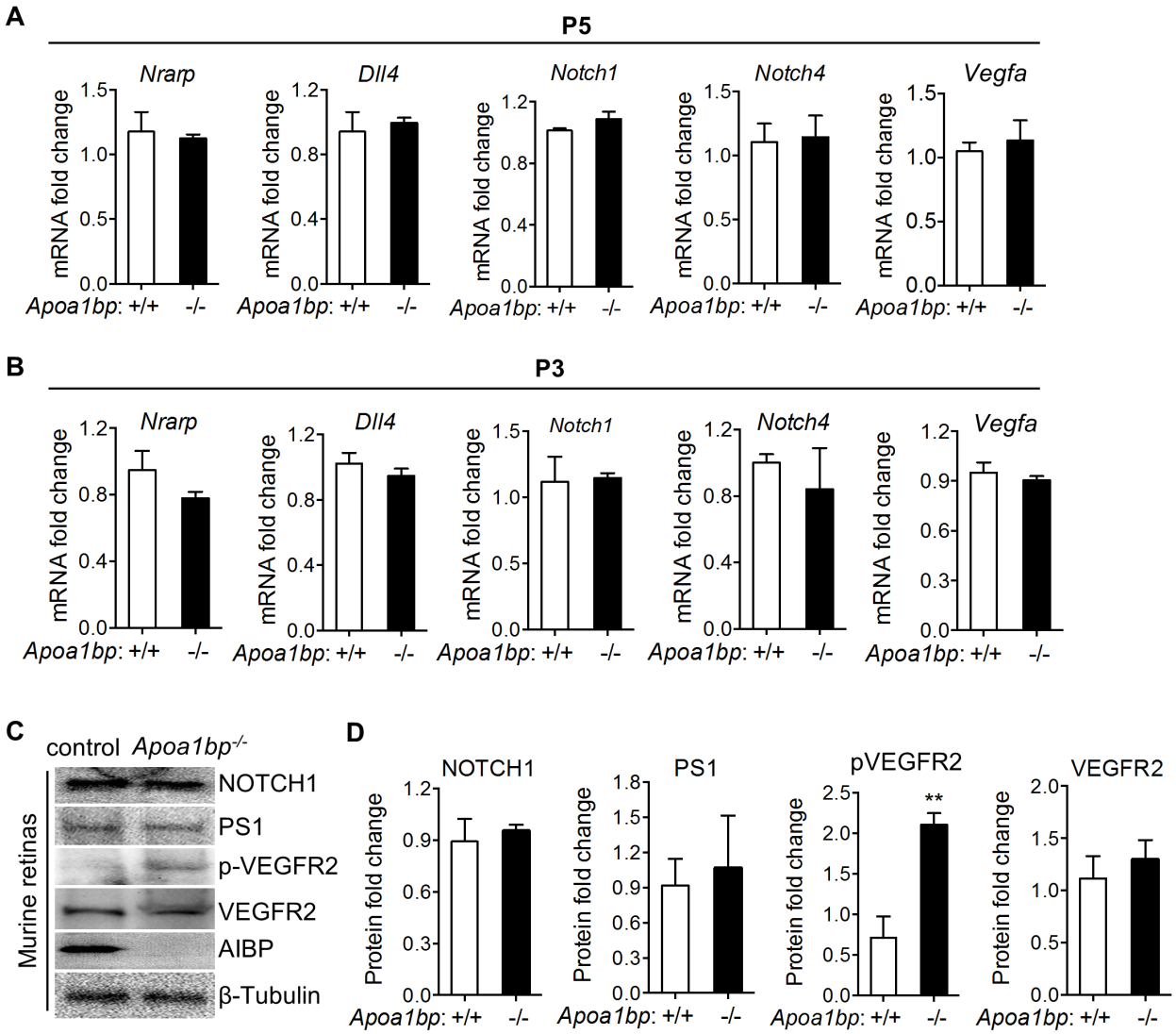

Online Figure V. Characterization of Notch pathway in the retinas of P5 AIBP knockout neonatal mice and their control littermates. Quantitative RT-PCR analysis of the Notch downstream mediator gene *Nrarp*, the Notch ligands *Dll4*, the Notch receptor *Notch1*, *Notch4* as well as *Vegfa* mRNA in P5 (A) and P3 (B) retinas from *Apoa1bp*$^{-/-}$ mice or control littermates. (C) Western blot of Notch1, PS1, p-VEGFR2 (Tyr1175) and VEGFR2 expression. Mean ± SD; n=3. **, $p<0.01$.

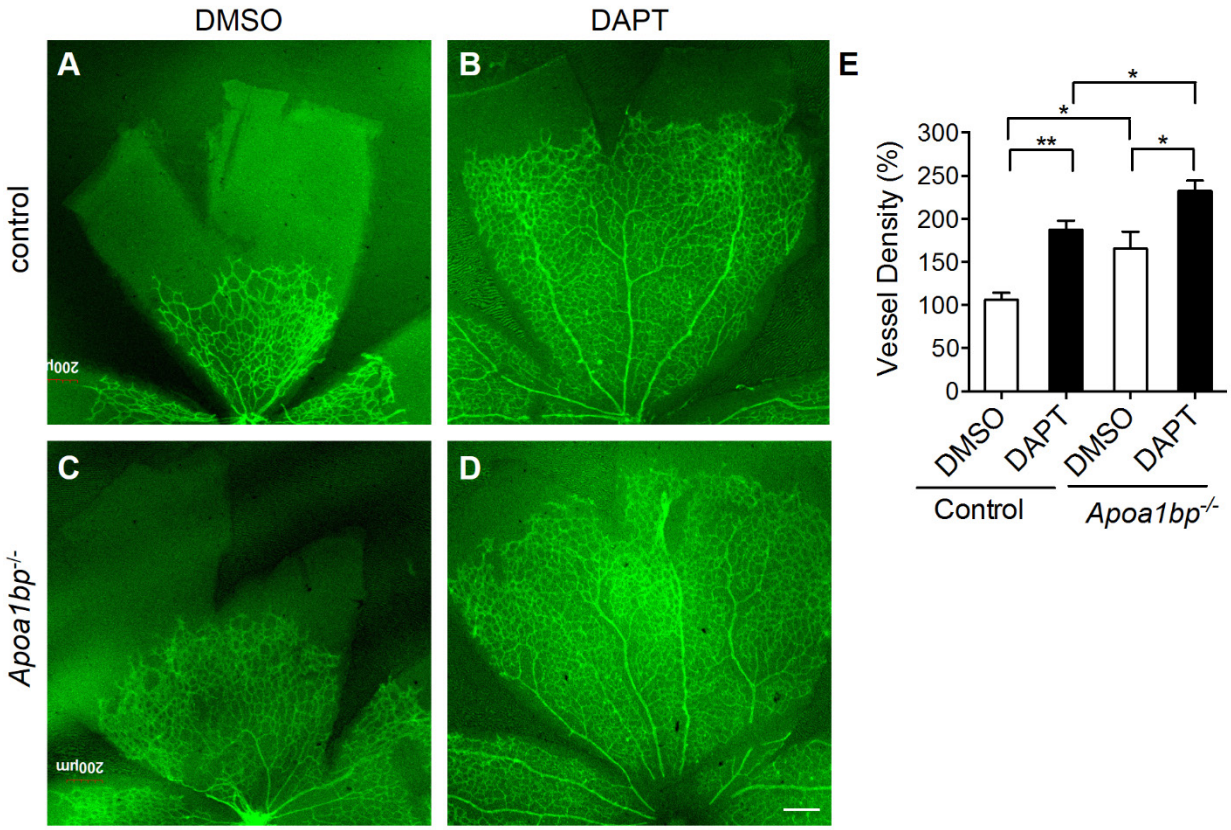

Online Figure VI. AIBP regulates Notch-dependent and –independent retinal angiogenesis. Control or AIBP KO mice at P4 were treated with DAPT and retinal angiogenesis was analyzed at P5. Scale bar, 200 μm. Mean ± SD; n=3. *, $p<0.05$; **, $p<0.01$.

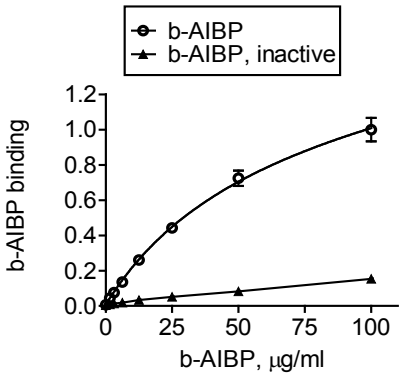

Online Figure VII. Binding of biotinylated AIBP (b-AIBP) to HRMECs. Confluent HRMECs were incubated with the indicated concentration of b-AIBP or inactive (heat-inactivated) AIBP for 2 hours at 4°C, and binding was assessed. A non-linear regression fit was applied to calculating the Kd ($2.1\pm0.3\times10^{-6}$ M). The data are representative of three independent repeats.

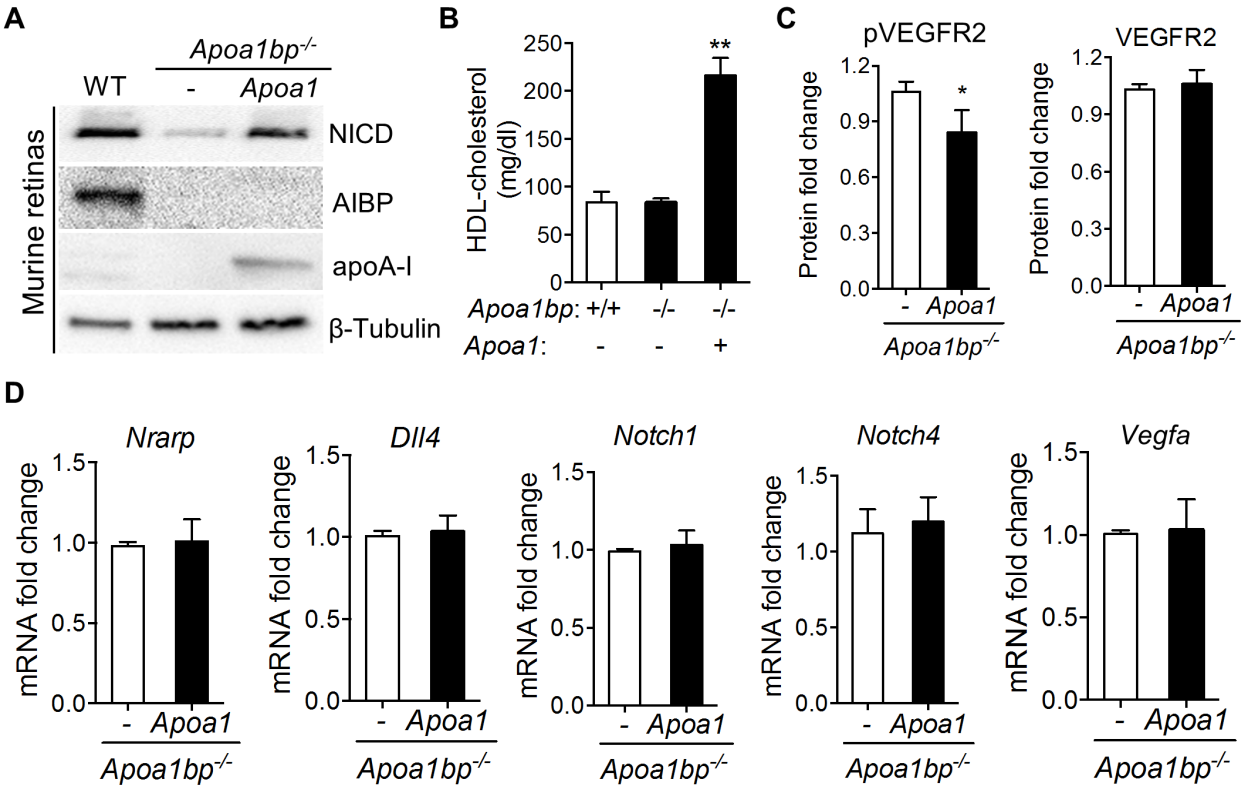

Online Figure VIII. Notch activity in the AIBP knockout retinas in the presence or absence of apoA-I overexpression. NICD protein expression (A), HDL-cholesterol concentration (B), VEGFR2 activation (C) and qRT-PCR analysis of *Nrarp*, *Dll4*, *Notch1*, *Notch4,* and *Vegfa* mRNA levels (D) in the retinas of *Apoa1bp*$^{-/-}$*Apoa1*^{Tg} and control *Apoa1bp*$^{-/-}$ mice at P5. Mean ± SD; n=3. **, p<0.01.

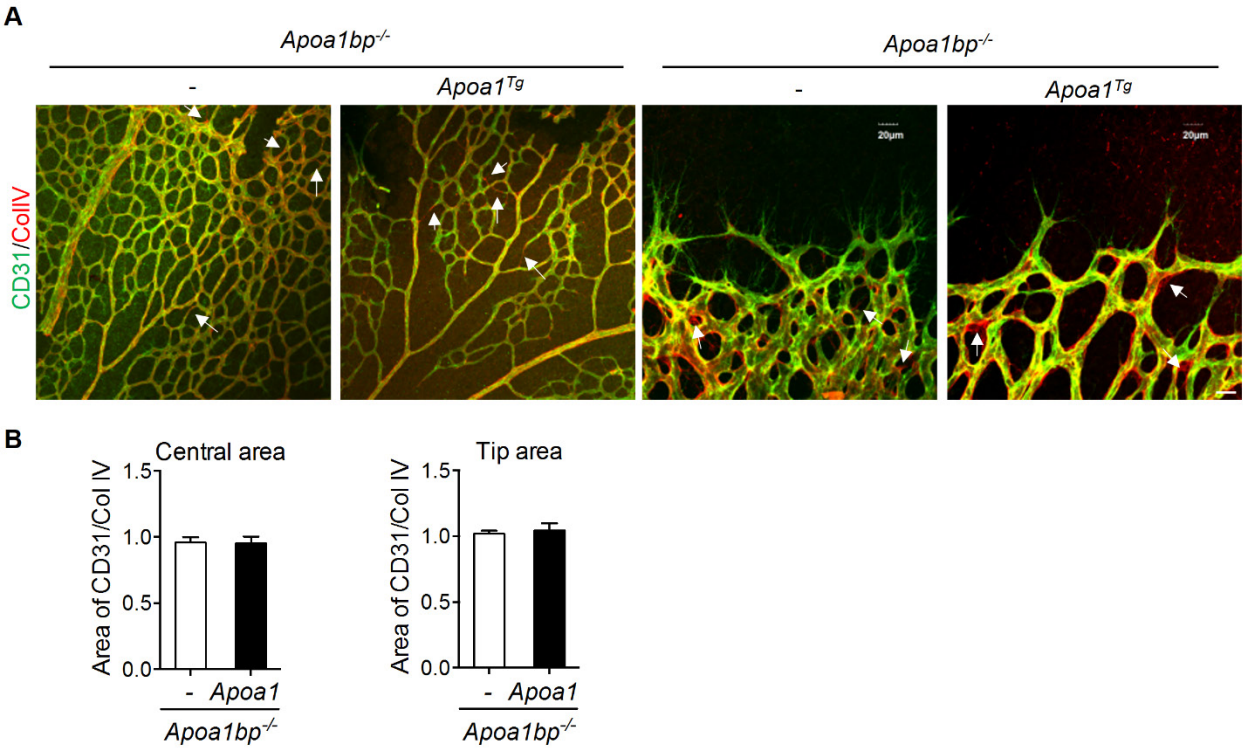

Online Figure IX. Similar vascular remodeling in Apoa1bp$^{-/-}$ and Apoa1bp$^{-/-}$ ×Apoa1^{Tg} mice.
(A) Images of whole mount immunostaining of P5 retinas from Apoa1bp$^{-/-}$ and control littermates using CD31 (green) and Col IV (red) antibodies. (B) CD31^{+} vs. Col IV^{+} area were compared. No obvious difference of vascular remodleing between *Apoa1bp*$^{-/-}$ and *Apoa1bp*$^{-/-}$ ×Apoa1^{Tg} retinas were found. Scale bar, 20 μm. Mean ± SD; n=3.

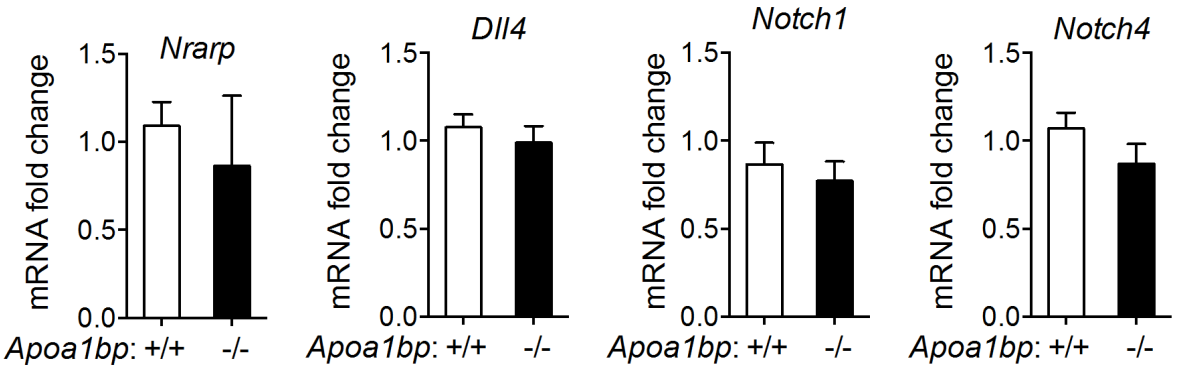

Online Figure X. AIBP effect on Notch signaling during neovascularization in the Matrigel plugs. Quantitative RT-PCR analysis of the Notch target gene *Nrarp*, *Dll4*, *Notch1*, and *Notch4* mRNAs in the Matrigel plugs from *Apoa1bp*$^{-/-}$ or control mice. Mean ± SD; n=3.

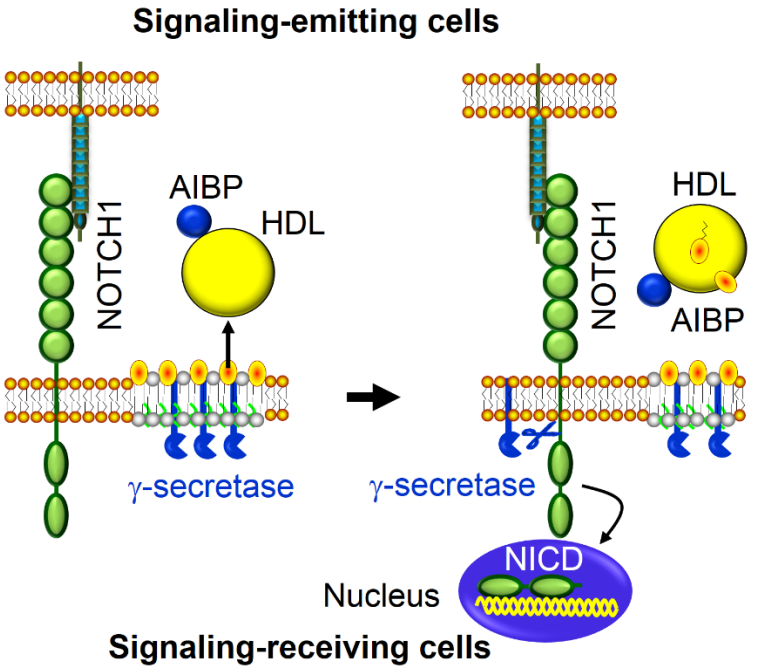

Online Figure XI. The model illustrates AIBP regulation of Notch signaling.
AIBP treatment accelerates cholesterol efflux from ECs to HDL, which disrupts lipid rafts and relocates Notch1 and γ-secretase from lipid rafts to non-lipid rafts, where increased co-distribution of the Notch receptor with γ-secretase will occur thus increasing Notch cleavage to generate NICD and subsequent signaling.

Online References

1. Gu Q, Yang X, Lin L, Li S, Li Q, Zhong S, Peng J and Cui Z. Genetic ablation of solute carrier family 7a3a leads to hepatic steatosis in zebrafish during fasting. *Hepatology*. 2014;60:1929-41.
2. Yang X, Gu Q, Lin L, Li S, Zhong S, Li Q and Cui Z. Nucleoporin 62-like protein activates canonical Wnt signaling through facilitating the nuclear import of beta-catenin in zebrafish. *Mol Cell Biol*. 2015;35:1110-24.
3. Mao RF, Rubio V, Chen H, Bai L, Mansour OC and Shi ZZ. OLA1 protects cells in heat shock by stabilizing HSP70. *Cell Death Dis*. 2013;4:e491.
4. Mills GL, Lane PA and Weech PK. *A guidebook to lipoprotein technique*. Amsterdam: Elsevier; 1984.
5. Fang L, Harkewicz R, Hartvigsen K, Wiesner P, Choi SH, Almazan F, Pattison J, Deer E, Sayaphupha T, Dennis EA, Witztum JL, Tsimikas S and Miller YI. Oxidized cholesteryl esters and phospholipids in zebrafish larvae fed a high cholesterol diet: macrophage binding and activation. *J Biol Chem*. 2010;285:32343-51.
6. Fang L, Choi SH, Baek JS, Liu C, Almazan F, Ulrich F, Wiesner P, Taleb A, Deer E, Pattison J, Torres-Vazquez J, Li AC and Miller YI. Control of angiogenesis by AIBP-mediated cholesterol efflux. *Nature*. 2013;498:118-22.
7. Li JL, Sainson RC, Shi W, Leek R, Harrington LS, Preusser M, Biswas S, Turley H, Heikamp E, Hainfellner JA and Harris AL. Delta-like 4 Notch ligand regulates tumor angiogenesis, improves tumor vascular function, and promotes tumor growth in vivo. *Cancer Res*. 2007;67:11244-53.
8. Hu J, Popp R, Fromel T, Ehling M, Awwad K, Adams RH, Hammes HP and Fleming I. Muller glia cells regulate Notch signaling and retinal angiogenesis via the generation of 19,20-dihydroxydocosapentaenoic acid. *J Exp Med*. 2014;211:281-95.
9. Kim J, Oh WJ, Gaiano N, Yoshida Y and Gu C. Semaphorin 3E-Plexin-D1 signaling regulates VEGF function in developmental angiogenesis via a feedback mechanism. *Genes Dev*. 2011;25:1399-411.
10. Jones A, Kumar S, Zhang N, Tong Z, Yang JH, Watt C, Anderson J, Amrita, Fillerup H, McCloskey M, Luo L, Yang Z, Ambati B, Marc R, Oka C, Zhang K and Fu Y. Increased expression of multifunctional serine protease, HTRA1, in retinal pigment epithelium induces polypoidal choroidal vasculopathy in mice. *Proc Natl Acad Sci U S A*. 2011;108:14578-83.
11. Kumar S, Berriochoa Z, Ambati BK and Fu Y. Angiographic features of transgenic mice with increased expression of human serine protease HTRA1 in retinal pigment epithelium. *Invest Ophthalmol Vis Sci*. 2014;55:3842-50.
12. Sayed N, Wong WT, Ospino F, Meng S, Lee J, Jha A, Dexheimer P, Aronow BJ and Cooke JP. Transdifferentiation of human fibroblasts to endothelial cells: role of innate immunity. *Circulation*. 2015;131:300-9.
13. Huang NF, Niiyama H, Peter C, De A, Natkunam Y, Fleissner F, Li Z, Rollins MD, Wu JC, Gambhir SS and Cooke JP. Embryonic stem cell-derived endothelial cells engraft into the ischemic hindlimb and restore perfusion. *Arteriosclerosis, thrombosis, and vascular biology*. 2010;30:984-91.